Journal of the European Ceramic Society **6** (1990) 169–177

Multiaxial Strength and Stress Rupture of Hot Pressed Silicon Nitride

George D. Quinn* & Günter Wirth

Institut für Werkstoff-Forschung, Deutsche Forschungsanstalt für Luft- und Raumfahrt, D 5000 Köln, FRG

(Received 16 August 1989; revised version received 14 February 1990; accepted 23 March 1990)

Abstract

The equibiaxial static fatigue resistance of hot pressed silicon nitride was measured at high temperature. A concentric ring scheme was used to load disks at up to 1300°C in air. Equibiaxial lifetimes were substantially shorter than uniaxial lifetimes, primarily a consequence of a drastically reduced biaxial strength. The static fatigue trends were similar in uniaxial and biaxial loading. The ring-on-ring scheme is not suitable for stress rupture testing if creep deformations are present or cracks grow large without going critical.

Das Versagen von heißgepreßtem Siliziumnitrid wurde bei hoher Temperatur unter symmetrischer, zweiachsiger Belastung mit konstanter Last gemessen. Die scheibenförmigen Proben wurden in Luft bis zu 1300°C durch eine Anordnung konzentrischer Ringe belastet. Zweiachsig mit symmetrisch verteilter Last bestimmte Lebensdauern waren wesentlich kürzer als einachsig bestimmte Lebensdauern was hauptsächlich eine Konsequenz der im zweiachsigen Fall drastisch reduzierten Festigkeit ist. Die Versagenstendenz unter konstanter Last war für einachsige und zweiachsige Belastung ähnlich. Die Ring-auf-Ring Anordnung ist bei vorhandener Kriechverformung oder im Fall groß wachsender Risse, die nicht kritisch werden, für Festigkeitsuntersuchungen ungeeignet.

On a mesuré la résistance en fatigue statique equibiaxiale à haute température d'un nitrure de silicium pressé à chaud. Des disques ont été contraints par des anneaux concentriques dans l'air à des températures allant jusqu'à 1300°C. Les tendances observées sont les mêmes que sous charge uniaxiale. Cependant, les durées de vie mesurées lors de ces essais sont nettement inférieures à celles mesurées sous charge uniaxiale, principalement en raison de la forte réduction de la résistance biaxiale. Le dispositif anneau–anneau n'est pas applicable à la mesure des contraintes de rupture s'il existe des déformations par fluage ou si les fissures se développent sans atteindre la taille critique.

* To whom all correspondence should be addressed at: National Institute for Standards and Technology, Ceramics Division, Gaithersburg MD, USA.

Introduction

Static fatigue failure of structural ceramics can be caused by a variety of phenomena including stress corrosion, slow crack growth, surface pit formation and creep fracture.[1] Hot pressed silicon nitride (HPSN) with magnesia sintering aid has been extensively studied due to its extremely consistent behavior.[2] Slow crack growth from preexisting flaws, or creep fracture can control static fatigue in HPSN.[3–6] An extensive data base of flexural stress rupture experiments has culminated in a fracture mechanism map as shown in Fig. 1.[3,5]

The vast majority of static fatigue experiments for engineering ceramics have been in a uniaxial stress state, indeed usually in four point flexure. Two studies have compared uniaxial and biaxial slow crack growth for alumina, glass and a glass ceramic[7,8] and a vitreous bonded abrasive.[9] Testing was only at room temperature, and with short duration, dynamic fatique experiments. These studies were encouraging however, showing that the multiaxial stress state had no effect upon crack growth parameters determined by strength test methods.

Journal of the European Ceramic Society 0955-2219/90/$3.50

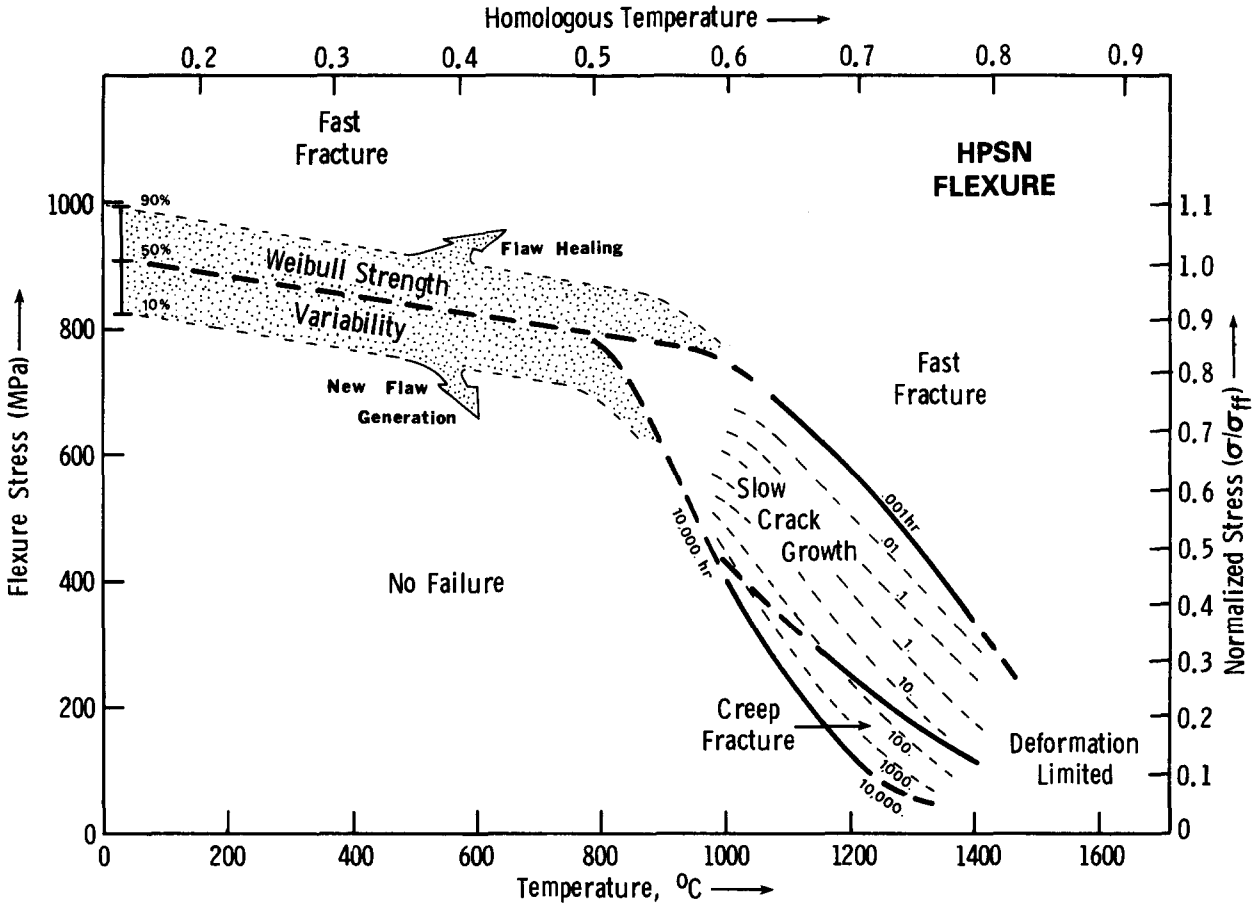

Fig. 1. Flexure fracture mechanism map for HPSN.[3,4]

This study reports high temperature, long duration equibiaxial stress rupture experiments for HPSN. HPSN was chosen because of its high static fatigue reproducibility. It was possible to examine more than one failure mechanism.[3,4] The biaxial results are directly compared to comprehensive uniaxial results from Refs 3, 4 and 10. Biaxial testing was performed in both the slow crack growth and creep fracture regimes. Preliminary findings of this study have been presented previously.[11] The present paper gives a more detailed interpretation, comprehensive fractography and the final conclusions of the study.

Material

The HPSN was NC 132 grade and was made in 1977 (Norton Co., Worcester, MA, USA). This material has a magnesia sintering aid and has been previously characterized.[10,12] Disk specimens were cut from a single plate identified as billet L. This was made from the same powder lot and was pressed at the same time as billets A, C and P described previously[3,4] Strength limiting defects in this material are typically machining damage from surface grinding, and tungsten carbide or disilicide inclusions.[12,13]

Experimental procedure

Thirty disks were prepared with 45 mm diameter and 2·2 mm thickness. The disks were prepared by conventional slicing and diamond grinding, but with special care to minimize machining damage in the final steps. The disks were then intended to be lapped very flat and to a depth of 25 μm from each side. The 25 μm is far greater than is necessary to produce a mirror finish, and was designed to eliminate typical machining damage inherent to the grinding process. This machining damage is anisotropic[14] and as such, would confound interpretation of biaxial effects on randomly dispersed flaws.

Seventeen flexure specimens of size 2·1 mm × 2·8 mm × 45 mm were prepared from the same billet in order to be broken at room temperature for a comparison of uniaxial to biaxial fast fracture strengths. The specimens were given the same grinding and lapping preparations as the disks. They were tested on MIL STD 1942(MR) compatible

flexure fixtures, which had 20·0 and 40·0 mm spans The nonstandard specimen size was used to permit ready comparison to earlier results.[3,4,10]

These precautions were taken to ensure the strength limiting flaws were identical in uniaxial and biaxial specimens. Giovan and Sines[15] found such precautions necessary in their study of uniaxial and biaxial strengths of alumina.

The biaxial fixtures are shown schematically in Fig. 2. Loading was via a ring-on-ring jig which produces an equibiaxial stress state. The rings were made from tubes of high purity recrystallized silicon carbide (Crystar Grade, Norton Co., Worcester, MA). This material was chosen because of its high refractoriness and ready availability in tube form. Indeed, after all experiments, the appearance of the SiC had hardly changed and there was no chemical reaction evident at the load points. The top of each tube was crowned with a radius such that the support (outer) ring had a nominal diameter of 40 mm and the loading (inner) ring 10 mm. A silicon nitride ball with a flat was used to apply the load centrally to the loading ring. The assemblage was aligned at room temperature and held in place by tack beads of a household acetate cement which subsequently burned off.

Deflection was measured from the midpoint relative to the outer ring. A silicon nitride ball

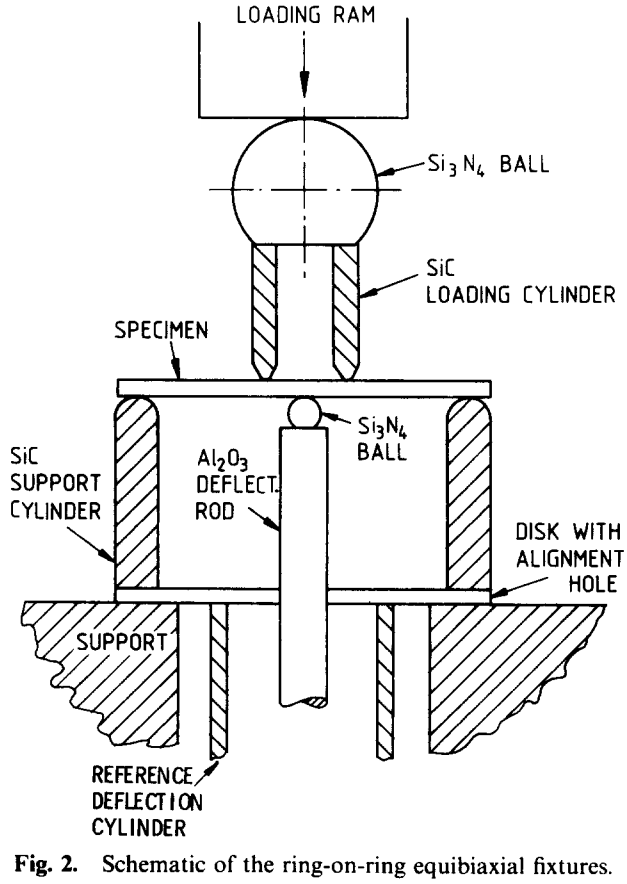

Fig. 2. Schematic of the ring-on-ring equibiaxial fixtures.

touched the specimen underside in order to ensure no contamination and a point contact. The outer ring and middle point deflections were transmitted to a LVDT outside the furnace.

Stress rupture experiments were performed in a SiC resistance heating furnace equipped with a dead weight lever arm system (Netzsch High Temperature Flexure Strength Tester Model 422). The load was accurate to within 1%. Temperature was stabilized for 15–30 min prior to load application, which took 5–10 s (the uniaxial specimens needed only 5 min to stabilize[10]). Temperature, which was held to within 3°C, was monitored by platinum thermocouple located 2 mm above the specimen.

Six specimens were broken to determine a reference strength at room temperature. A screw-driven universal testing machine (Instron Model 1195, Canton, MA, USA) was used at a crosshead rate of 0·5 mm/min causing failures in 20–30 s.

All stresses were computed from the elastic stress formula:[15–17]

$$\sigma = \frac{3p}{2\pi h^2}\left[(1-\nu)(a^2-r^2)\Big/ 2b^2 + (1+\nu)\,ln\left(\frac{a}{r}\right)\right]$$

where b is the specimen radius, a the radius of the support ring, r the load ring radius, h the specimen thickness, p the load. Poisson's ratio ν was taken to be 0·26 at room temperature and 0·19 at 1200 and 1300°C.[18]

The specimen and fixture sizes were chosen on the basis of the following criteria. First, it was desired to eliminate specimen size effects upon strength. The disks should have the same volume or area under maximum load, with a similar through-the-thickness stress gradient, so as to have similar Weibull effective surfaces or volumes. Secondly, since the loading rings were made of a refractory but weak ceramic, absolute load levels had to be kept low. Next, friction errors in loading which could not entirely be eliminated (very difficult with high temperature fixtures) had to be comparable between the four point and disk tests. Frictional constraint at the fixed load points can lead to errors of the order of 1–20% in stress in both four point flexure[19] and in disk testing.[16] In both cases the friction error is directly proportional to the coefficient of friction (difficult to control at high temperature) and the specimen thickness. Giovan and Sines,[20] minimized friction error in their low to moderate temperature ring on ring apparatus by use of crowned loading rings and lapped specimens. Both steps were used in this study for the disks, but since the coefficient of high temperature friction could not be controlled, the uniaxial and biaxial specimen thicknesses were kept

similar so as to keep the parasitic friction moments comparable. Consideration of possible stress relaxations due to creep relaxation was a further motivation to use the same specimen thickness. These factors together led to a choice of disk thickness of 2·2 mm which is similar to the 2·1–2·3 mm flexure bar thicknesses used for the uniaxial stress rupture data base.[3,4]

The four point spans had been of the order of 40 mm × 20 mm, but such dimensions for the ring diameters in biaxial loading would have required very high loads. Thus, an outer diameter of 40 mm was used but with an inner diameter of 10 mm. The area in the inner ring which has constant stress is thus 79 mm^2 which is comparable to the 56 and 71 mm^2 areas in the four point specimens from the earlier studies.

Finally, the error due to wedging stresses (due to excessive concentrated stresses under the loading ring) was minimized as a consequence of the system geometry. The absolute load to cause breakage was about ten times greater in the disk specimen, but the inner ring had six times more contact length, so the distributed load and thus the wedging stresses were comparable and rather low.

All of these preparations were successful as the fixtures were never damaged. The specimens broke in an ideal fashion, almost always within the middle gage area, and not under the load circle. So in summary, the disk ring-on-ring test configuration is in essence a two-dimensional flexure test. As much as possible, testing conditions were chosen to permit a direct comparison to the one-dimensional, uniaxial flexure test.

Results

The six disks broken at room temperature had an average strength of 501 MPa and a standard deviation of only 29. A Weibull two-parameter analysis† gave a modulus of 19 (Fig. 3). Five of the fractures originated inside the gage area, the sixth outside. Figure 4 shows one of the former. Failure origins were readily observable based upon the crack branching patterns. Scanning electron microscopy unfortunately identified the strength limiting flaws in several specimens to be subsurface machining damage (Fig. 5(a)). Such damage appeared as 15–20 μm deep elongated semielliptical cracks which

† Least squares analysis with probability of failure equal to $(i - 0{\cdot}5)/n$ where i is the ith data point, and n the total number of specimens.

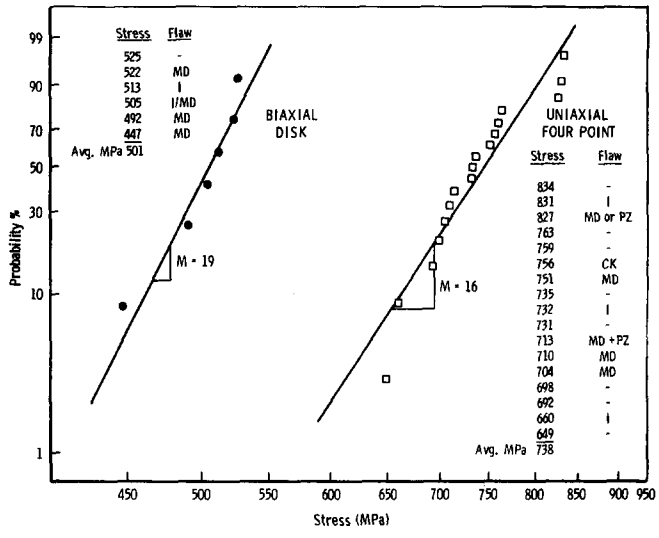

Fig. 3. Room temperature uniaxial and biaxial strengths. In the flaw key, I denotes an inclusion; MD, machining damage, PZ, a porous zone and '—' is uncertain.

often overlapped. These occasionally intersected at different angles creating a zig-zag defect at the failure origin. This was presumably due to a shift in orientation of the specimen during surface grinding. Inclusions caused failures in at least one specimen. A mounting clay contamination problem obscured the origins in the others.

The equibiaxial strength (501 MPa) is substantially lower than the 738 MPa (±53 MPa) uniaxial strength which was measured on the 17 flexure bars. The uniaxial flexure, Weibull two-parameter modulus was 16 but could have been higher with the deletion of a few *high* strength points (Fig. 3). Strength limiting flaws again were either 15–25 μm deep semielliptical machining damage or tungsten

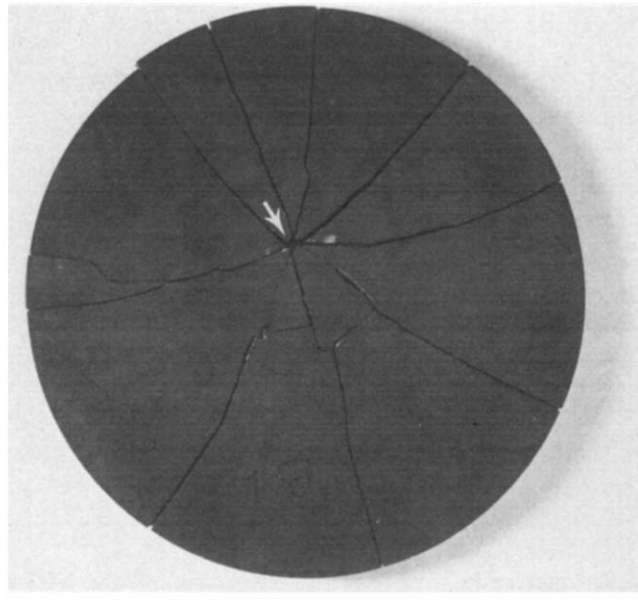

Fig. 4. Disk specimen fracture at room temperature at 492 MPa. The arrow marks the failure origin.

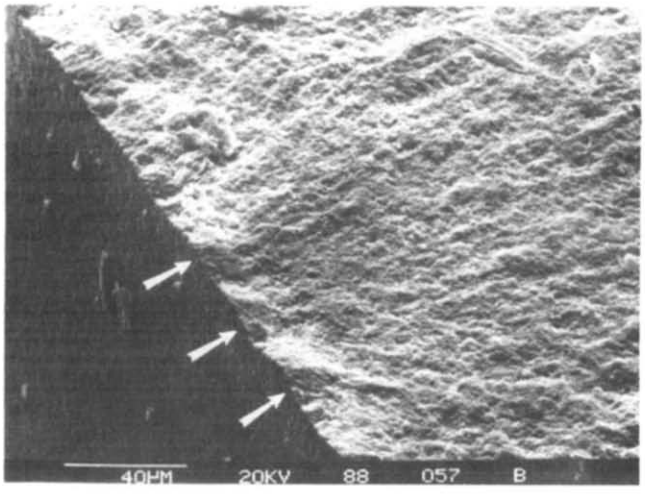

(a)

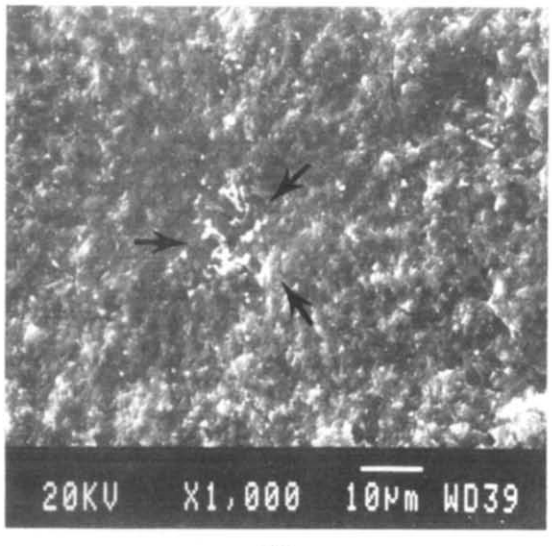

(b)

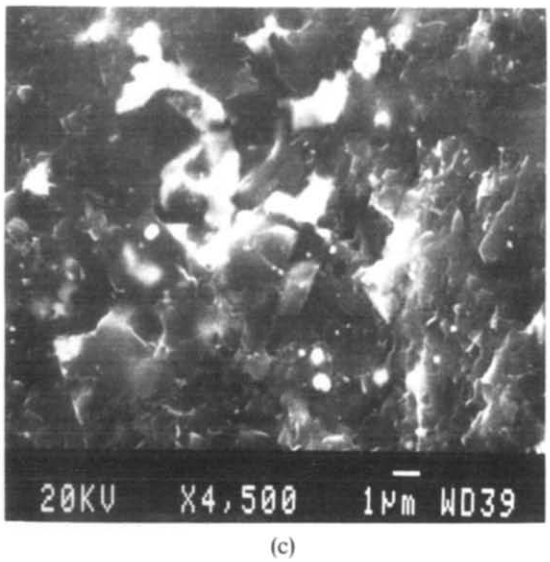

(c)

Fig. 5. Fracture origin in disk and flexure specimens. (a) Zig-zag machining damage as verified by radiating hackle. The particle in the upper left is a contaminant (b), (c) A tungsten carbide or silicide inclusion.

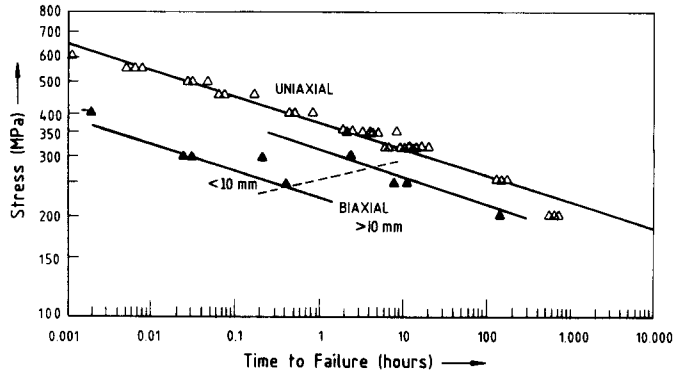

Fig. 6. Biaxial stress rupture data (solid symbols) at 1200°C in air for HPSN. The limits of the biaxial results are shown by lines. Uniaxial results (hollow points) are given for comparison. The arrowed points are either failures on loading or an interrupted test. The dashed line marks where SCG zones extended beyond the 10 mm central load region.

inclusions. These inclusions typically were small broken-up particles (Figs 5(b) and 5(c)). They were *smaller* than comparable strength semicircular penny shaped defects, a consequence of a locally reduced fracture toughness.[13]

The stress rupture results at 1200°C are shown in Fig. 6. Biaxial lifetimes appear to be considerably shortened but with high scatter relative to uniaxial stress rupture results taken from Refs 2–4). Figures 7 and 8 show crack patterns in these specimens. The short duration specimens (<0·2 h) had small intergranular slow crack growth (SCG) zones (100–500 μm size) changing to a transgranular fast fracture crack. Longer-lived specimens had much larger crack growth zones. For example, the 250 MPa specimen at 0·4 h had a 10 mm-long SCG region. Large SCG zones in four point flexure specimens are also possible,[12] but not as large as 10 mm. It must also be remembered the uniform stress zone in the disk specimen is only 10 mm in diameter. Outside the inner loading ring, the radial and tangential stresses diminish rapidly (the radial stresses the more so).[16,17]

The 1300°C biaxial results (Fig. 9) seem to be more clear since scatter in lifetime is dramatically reduced. Overall lifetime is shortened by a factor of about 20, but the static fatigue trend is comparable to the uniaxial results. The slope of a line through the biaxial results gives a SCG exponent of 8·4, whereas the uniaxial exponent is 9·9 (stress = constant × (time to failure)$^{-1/N}$; where N is the slow crack growth exponent[2,10]). The SCG zones at 1300°C were much larger and more severe than at 1200°C. Even the short duration specimens had large zones of the order of 10 mm length, which extended completely through the thickness. The specimens loaded at 200 MPa or less had SCG zones extending

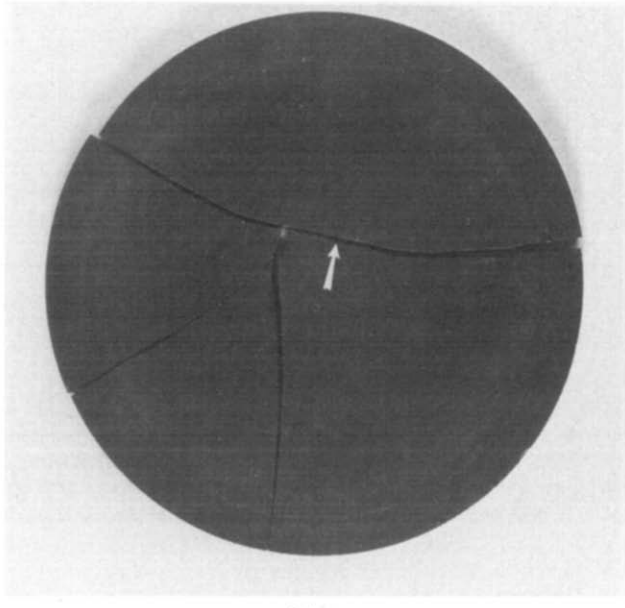

(a)

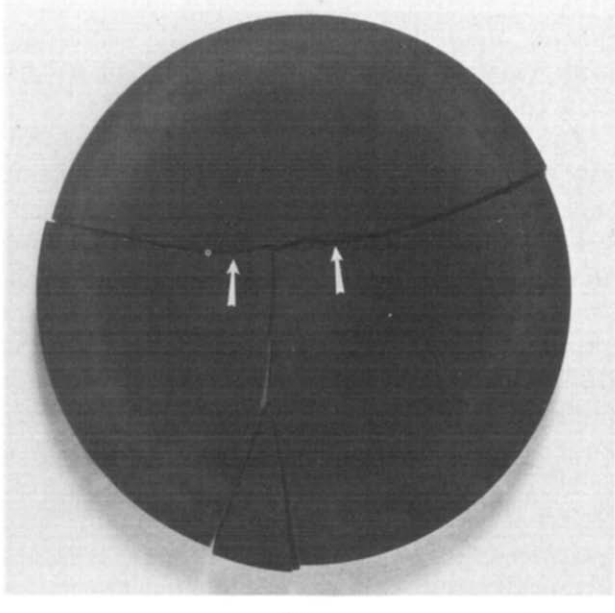

(b)

Fig. 7. Disk stress rupture specimens. (a) Specimen which failed at 1200°C after 0·2 h with 300 MPa. The SCG Zone was 1 mm long. (b) Disk specimen that failed at 1200°C after 2·5 h. The SCG Zone was 8 mm long (arrows).

to the *outer* load ring and even to the specimen rim. This is very unfortunate and it is clear that, with the exception of the first three specimens, the cracks in the specimen were typically moving through regions of nonuniform stress in the specimen. The last three specimen failures were due to creep fracture only and not slow crack growth as well.

Discussion

It is disheartening to observe that, after what apparently were careful precautions, machining

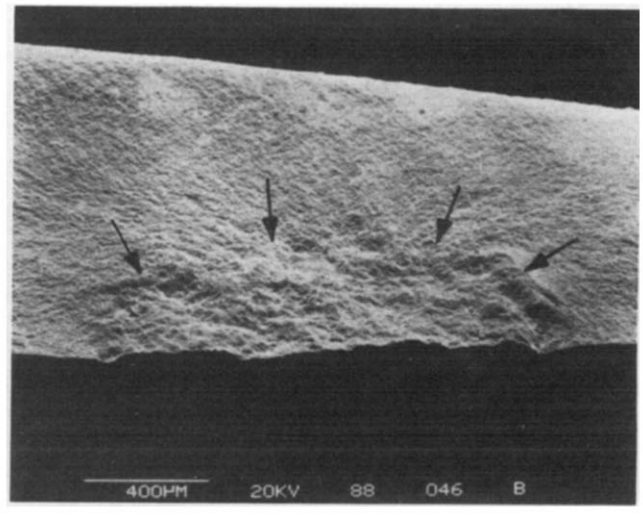

Fig. 8. SEM photo of the fracture surface of the 1200°C specimen shown in Fig. 7(a).

damage persisted in both the bend bars and the disks. The machining damage was centered on, or exacerbated by, the presence of 1–3 μm-sized pores in the material, which is to say failure occurred from machining damage that may have interacted with natural microdefects. The zig-zag, interactive machining damage in the disks could prove to be diabolical to analyze. Most previous studies, wherein machining damage was inferred as an interfering factor in disk specimens, did not actually verify it (e.g. Ref. 15). In the present case the machining vender, a reliable establishment, subcontracted the tedious lapping to another shop and the work was not done to specification. Only a few micrometers were removed, which produced a pretty 25–50 nm (1–2 rms microinch) surface, but only managed to conceal the subsurface cracks (15–20 μm). The 32% reduction in fast fracture strength from uniaxial to biaxial loading therefore has to be considered in the context of the statistics of machining damage variability (and not in the

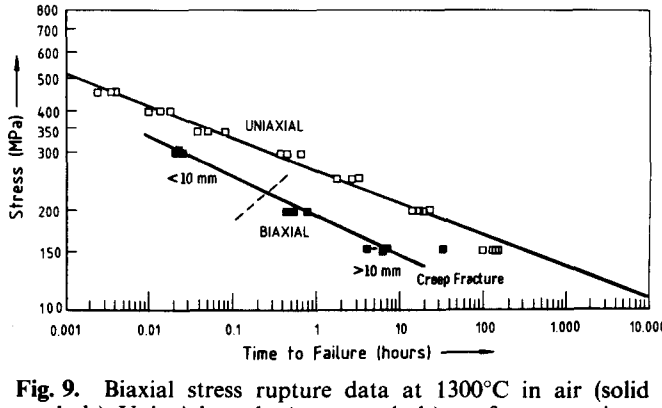

Fig. 9. Biaxial stress rupture data at 1300°C in air (solid symbols). Uniaxial results (open symbols) are for comparison. The dashed line marks the limit where SCG zones extended beyond the 10 mm central load region.

context of randomly oriented, noninteractive idealized defects). Most studies, both analytical and experimental, suggest equibiaxial weakening will be of the order of 5–20%.[21–24] Almost all of these studies are clouded by experimental uncertainties (friction errors, uniaxial biaxial size effects or no fractography). We are unable to distinguish how much of the 32% reduction in the present study is due to equibiaxial weakening, and how much is due to flaw population variation.

The reduction in stress rupture lifetime for biaxial loading is not surprising. The slow growth cracks followed a very tortuous and winding path at both 1200 and 1300°C, and numerous multiple crack patterns, even cracks growing at 90° relative to each other were observed. The cracks seemed to be active in all directions. The irregularity of the cracks suggest extensive microcrack interactions, or possibly the ability to circumvent pockets of resistance. Such crack freedom was noted by Pletka and Wiederhorn in their comparison of uniaxial and biaxial crack growth behavior.[8] Although the biaxial lifetimes seem to be shorter, this may simply be a consequence of the dramatically reduced fast fracture strength (501 MPa) of the biaxial specimens. Indeed, if the data in Figs 6 and 9 are normalized by the reference strengths at room temperature, then the static fatigue curves are comparable, and there is no biaxial lifetime shortening. (The biaxial stress rupture results are normalized by the fast fracture data of this report (501 MPa). The uniaxial stress rupture data, if normalized by the fast fracture strength (738 MPa) of this report, will overlap. Alternatively, if the uniaxial strength from Ref. 10 (909 MPa, where the flexure stress rupture data are first reported) is used, then the biaxial curve would actually shift higher. These latter fast fracture results are atypically high for this HPSN however, as noted in Ref. 10.)

The similarity in static fatigue strength degradation in biaxial and uniaxial modes of loading is reassuring since it would lead to simplified life prediction models. Service and Ritter[9] have also reported identical static fatigue susceptibilities in uniaxial and biaxial stress states. Pletka and Wiederhorn[7,8] showed consistent susceptibilities in uniaxial and biaxial disk strength testing as well.

These sanguine interpretations must be tempered by some serious experimental shortcomings however. The first complicating factor is the large crack sizes in many of the biaxial specimens of the present study. These behaved in many respects like fracture mechanics specimens (such as double torsion). Double torsion experiments at 1200 and 1300°C on the identical material were reported previously by this author.[10] A striking similarity in the scatter of results was reported: high variability at 1200°C, good consistency at 1300°C. Variable zones of crack growth resistance were also reported.[10] The crack fronts in the biaxial disk specimen (transition from SCG intergranular to fast fracture transgranular) were curved, much like fronts in double torsion specimens.

Whereas there was sufficient stored elastic energy in the biaxial fast fracture specimens to cause breakage once a flaw was critically loaded, this was not necessarily true in the stress rupture specimens which were at much reduced levels. Thus, a crack which had grown from a few micrometers to 10 mm may have accelerated to velocities in the 10^{-3} to 10^{-2} m/s range (which often is the highest practically measured velocities in static laboratory fracture mechanics tests), but then the crack could rapidly unload and decelerate as it reached the lower stressed region between the inner and outer rings. The specimens where the crack growth markings extend much outside the inner ring therefore, have to be regarded with skepticism. These are so noted in Figs. 6 and 9. The fracture times can at best be considered overestimated.

The large cracks may have altered the specimen compliance as shown in Fig. 10. Indeed, it is a peculiar consequence of the ring-on-ring system, that as a crack grows in one direction the specimen will bend due to reduced compliance and thus, will redistribute the ring loading to effectively reduce the stresses acting on the plane of the crack. Figure 10 shows the loading rings will not evenly distribute the load as the specimen deflects preferentially in one direction.

Creep deformations are an additional complicating factor. Biaxial deformations often exhibit primary, secondary and tertiary stages. The latter was in the present case undoubtedly due to a compliance effect as cracks became extremely large. Secondary creep deformation rates were never constant and always decreased, indicating no true steady state. Primary rates were as high as 100 times faster than minimum rates. Overall deflections were of the order of 0·1–1 mm for most specimens. The analysis of the deformation to give strains and relaxed stresses would be extremely complicated. Several of these specimens were loaded in conditions of creep fracture. As an extreme example, the specimen loaded to 150 MPa at 1300°C was interrupted at 32 h, as it was well into a tertiary creep deformation mode, but just a moment before fracture. It had numerous creep cracks and a central

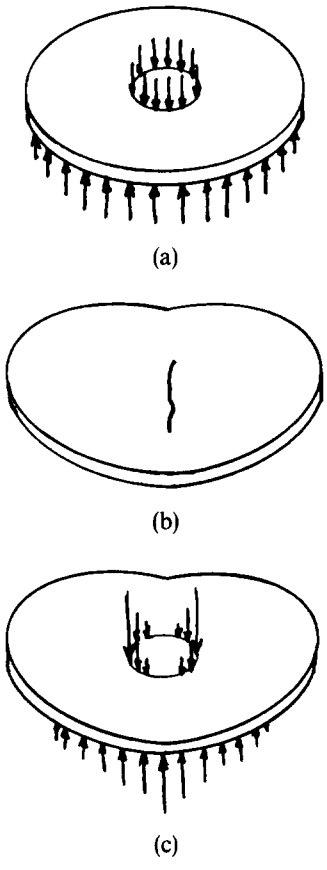

Fig. 10. A cracked specimen has a nonuniform compliance which causes uneven loading. (a) Flat specimen; uniform loading; (b) cracked specimen; compliance is different in different orientations; (c) resulting uneven loading.

plug was almost punched out under the loading ring (Fig. 11).

Finally, it was clear from the specimen fragments that creep and crack growth severely interfered with each other. That is, creep often blunted cracks and reduced stress intensities. Alternatively, crack growth created deformations that interfered with creep measurements.

Conclusions

1. The biaxial stress rupture lifetime of HPSN appears to be reduced compared to uniaxial lifetimes at high temperature. This is primarily due to a reduced fast fracture strength.

2. The biaxial fatigue trend of strength degradation appears to be the same as the uniaxial trend.

3. Biaxial SCG cracks wend a tortuous path through the specimen, unlike biaxial fast fracture or uniaxial cracks.

4. The fast fracture strength limiting defects were the same in the biaxial and uniaxial specimens: machining damage and tungsten carbide or silicide inclusions.

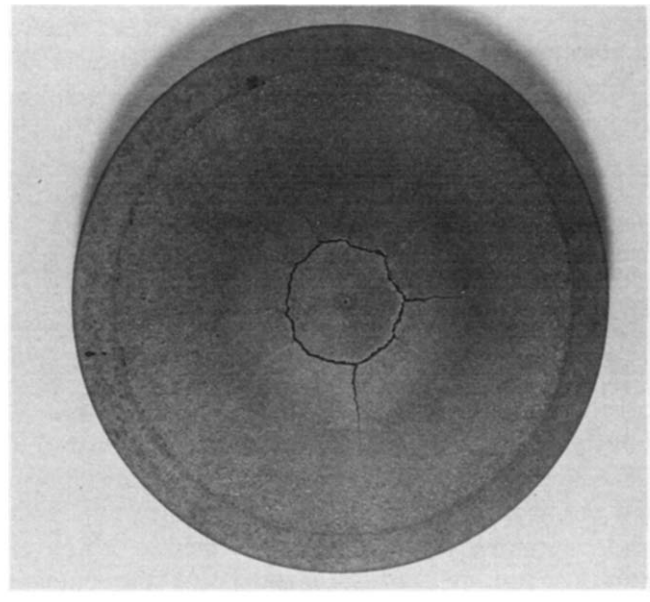

Fig. 11. Specimen exhibiting excessive creep deformation and localized creep cracking at 32 h at 1300°C with 150 MPa. The test was terminated just short of fracture when 'tertiary' creep was well underway.

5. The machining damage persisted despite careful specifications intended to remove it. The very pessimistic conclusions of Giovan and Sines[15] regarding machining damage should be amended to include: 'Careful specifications will not guarantee proper specimen preparation.'

6. The ring-loaded disk specimen exhibited a wide range of behavior. Some fractures were ideal strength (i.e. small crack, no creep) type specimens, others were like fracture mechanics (large crack) specimens, and finally some as creep fracture specimens. There was a tendency for stresses to redistribute as the compliance changed due to large crack growth.

7. The ring-loaded disk specimen should only be used for stress rupture experiments where crack sizes and deformations are small.

Acknowledgement

The principal author (GDQ) Wishes to thank Dr R. N. Katz of US Army MTL who suggested the experiment contained in this paper. The assistance of Mr Bernd Kanka of DLR and Ms Gail Meyers of MTL with scanning electron microscopy is appreciated.

References

1. Quinn, G., Review of static fatigue in silicon nitride and silicon carbide. *Ceram. Eng. & Sci. Proc.*, 3 (1987) 77–98.

2. Quinn, G. & Swank, L., Static fatigue of preoxidized hot pressed silicon nitride. *Comm. Amer. Ceram. Soc.*, Feb. (1983) C31–2.
3. Quinn, G., Static fatigue resistance of hot pressed silicon nitride. In *Fracture Mechanics of Ceramics, Vol. 8*, ed. R. Bradt, A. Evans, D. Hasselman & F. Lange. Plenum Press, New York, 1986, pp. 319–32.
4. Quinn, G., Fracture mechanism maps for silicon nitride. In *Ceramic Materials and Components for Engines*. ed. W. Bunk & H. Hausner, Deutsche Keramische Gesellschaft, Berlin, 1987, pp. 931–939.
5. Grathwohl, G., Regimes of creep and slow crack growth in high temperature rupture of hot pressed silicon nitride. In *Deformation of Ceramic Materials II*, ed. R. Tressler & R. Bradt. Plenum Press, New York, 1o84, pp. 513–87.
6. Grathwohl, G., Creep and fracture of hot pressed silicon nitride with natural and artificial flaws. In *Creep and Fracture of Engineering Materials and Structures*, ed. B. Wilshire & D. Owen. Pineridge Press, Swansea, 1984, pp. 565–77.
7. Pletka, B. & Wiederhorn, S., A comparison of failure predictions by strength and fracture mechanics techniques. *J. Mat. Sci.*, **17** (1982) 1247–68.
8. Pletka, B. & Wiederhorn, S., *Subcritical crack growth in glass ceramics*. In *Fracture Mechanics of Ceramics, Vol. 4*, ed. R. Bradt, D. Hasselman & F. Lange. Plenum Press, New York, 1980, pp. 745–59.
9. Service, T. & Ritter, J., Dynamic fatigue of a vitreous bonded abrasive tested in four point and ring-on-ring flexure. *Adv. Cer. Mat.*, **3** (1988) 49–51.
10. Quinn, G. & Quinn, J., Slow crack growth in hot pressed silicon nitride. In *Fracture Mechanics of Ceramics, Vol. 6*, ed. R. Bradt, A. Evans, D. Hasselman & F. Lange. Plenum Press, New York, 1983, pp. 603–36.
11. Quinn, G. & Wirth, G., Biaxial stress rupture of silicon nitride. *Mat. Sci. & Eng.*, **A109** (1989) 147–52.
12. Quinn, G., Characterization of turbine ceramics after long term environmental exposure. US Army AMMRC Technical Report TR 80-15, Watertown, Mass., USA, 1980.
13. Baumgartner, H. & Richerson, D., Inclusion effects on the strength of hot pressed Si_3N_4. In *Fracture Mechanics of Ceramics, Vol. 1*, ed. R. Bradt, D. Hasselman & F. Lange. Plenum Press, New York, 1974, pp. 367–86.
14. Rice, R. W., Freiman, S. W., Mecholsky, J. J., Jr, Rich, R. & Harada, Y., Fractography of Si_3N_4 and SiC. In *Ceramics for High Performance Applications II*, ed. J. Burke, E. Lence & R. Katz. Brook Hill, Chestnut Hill, MA, 1978, pp. 669–87.
15. Giovan, M. N. & Sines, G., Biaxial and uniaxial data for statistical comparisons of a ceramic's strength. *J. Am. Ceram. Soc.*, **62** (1979). 510–15.
16. Fessler, H. & Fricker, D. C., A theoretical analysis of the ring-on-ring loading disk test. *J. Am. Ceram. Soc.*, **67** (1984) 582–8.
17. Ritter, J. E., Jr, Jakus, K., Batakis, A. & Bandyopadhyay, N., Appraisal of biaxial strength testing. *J. Non Cryst. Solids*, **38** (1980) 419–24.
18. Kossowsky, R., Miller, D. G. & Diaz, E. S., Tensile and creep strengths of hot pressed Si_3N_4. *J. Mat. Sci.*, **10** (1975) 983–97.
19. Baratta, F. I., Quinn, G. D. & Matthews, W. T., Errors associated with flexure testing of brittle materials. US Army MTL Technical Report TR 87–35, Watertown, MA, July 1987.
20. Giovan, M. N. & Sines, G., Strength of a ceramic at high temperatures under biaxial and uniaxial tension. *J. Am. Ceram. Soc.*, **64** (1981) 68–73.
21. Weibull, W., Statistical theory of the strength of materials. *Ingenioersvetenskapsakad. Handl.*, No. 151, 1939, 45 pp.
22. Batdorf, S. D. & Heinisch, H. L., Jr, Weakest link theory reformulated for arbitrary fracture criterion. *J. Am. Ceram. Soc.*, **61** (1978) 355–8.
23. Evans, A. G., A general approach for the statistical analysis of multiaxial fracture. *J. Am. Ceram. Soc.*, **61** (1978) 302–8.
24. Rosenfield, A. R., Shetty, P. K. & Duckworth, W. H., Strength of ceramics subjected to biaxial stresses: II Combined normal loads (in preparation).